(21) G. M. Brown and W. D. K. Clark, unpublished work.
(22) The $[Ru(NH_3)_4(bpy)/Ru(NH_3)_4(phen)]^{3+/2+}$ electron transfer reaction has previously been studied in 1 M $HClO_4$.[12a] We have been unable to reproduce the rate constants reported in ref 12a.
(23) R. G. Wilkins and R. E. Yelin, *Inorg. Chem.*, 7, 2667 (1968).
(24) R. C. Young, F. R. Keene, and T. J. Meyer, *J. Am. Chem. Soc.*, **99**, 2468 (1977).
(25) R. A. Robinson and R. H. Stokes, "Electrolyte Solutions", 2nd ed., Academic Press, New York, N.Y., 1959, p 227.
(26) The computer program used to obtain the values of the constants was based on R. H. Moore and R. K. Zeigler, Los Alamos Scientific Laboratory Reports LA-2367, 1959, and P. McWilliams, LA-2367 Addenda, 1962. This program was generously supplied by Dr. T. W. Newton. Each rate constant was weighted according to its reciprocal.
(27) T. W. Newton, "The Kinetics of the Oxidation-Reduction Reactions of Uranium, Neptunium, Plutonium, and Americium in Aqueous Solutions", ERDA Critical Review Series, TID-26506, 1975.
(28) T. J. Meyer and H. Taube, *Inorg. Chem.*, 7, 2369 (1968).
(29) R. A. Marcus and N. Sutin, *Inorg. Chem.*, **14**, 213 (1975).
(30) D. K. Lavallee, C. Lavallee, J. C. Sullivan, and E. Deutsch, *Inorg. Chem.*, **12**, 570 (1973).
(31) C. Lavallee and D. K. Lavallee, *Inorg. Chem.*, **16**, 2601 (1977).
(32) M. Abe, G. M. Brown, H. J. Krentzien, and H. Taube, to be published.
(33) (a) M. Eigen, *Z. Phys. Chem. (Frankfurt am Main)*, 1, 176 (1954); (b) R. M. Fuoss, *J. Am. Chem. Soc.*, **80**, 5059 (1958).
(34) R. G. Wilkins, *Acc. Chem. Res.*, **3**, 408 (1970).
(35) The close-contact distance does, however, correspond to the maximum rate constant.
(36) H. C. Stynes and J. A. Ibers, *Inorg. Chem.*, **10**, 2304 (1971).
(37) W. P. Griffith, *J. Chem. Soc. A*, 899 (1966).
(38) M. E. Gress, C. Creutz, and C. O. Quicksall, unpublished work.
(39) D. E. Richardson, D. D. Walker, J. E. Sutton, and H. Taube, unpublished work.
(40) A. Zalkin, D. H. Templeton, and T. Ueki, *Inorg. Chem.*, **12**, 1641 (1973); J. Baker, L. M. Engelhardt, B. N. Figgis, and A. H. White, *J. Chem. Soc., Dalton Trans.*, 530 (1975).
(41) The calculations of ΔG_{in}^{*} are based on a harmonic potential energy surface and have not been corrected for the zero-point energy of the reactants. For the $Ru(NH_3)_6^{3+/2+}$ system, the contribution from the zero-point energy is ~0.6 kcal mol^{-1}.
(42) Using the "hard sphere" radii of the reactants, $\bar{r}$ is 6.9 Å for the $Fe(H_2O)_6^{3+/2+}$ exchange reaction. The Fe–Fe distance can be decreased to 5.5 Å without creating a H–H contact shorter than twice the van der Waals radius of an H atom (M. D. Newton, personal communication).
(43) H. Fischer, G. M. Tom, and H. Taube, *J. Am. Chem. Soc.*, **98**, 5513 (1976).
(44) K. Rieder and H. Taube, *J. Am. Chem. Soc.*, **99**, 7891 (1977).
(45) A. Ekstrom, A. B. McLaren, and L. E. Smythe, *Inorg. Chem.*, **15**, 2853 (1976).
(46) E. Waisman, G. Worry, and R. A. Marcus, *J. Electroanal. Chem.*, **82**, 9 (1977).
(47) N. S. Hush, *Prog. Inorg. Chem.*, **8**, 391 (1967).
(48) G. M. Tom, C. Creutz, and H. Taube, *J. Am. Chem. Soc.*, **96**, 7827 (1974).
(49) C. Creutz, *Inorg. Chem.*, 17, 3723 (1978).
(50) M. D. Newton, personal communication.
(51) Better agreement between the observed kinetic parameters and the values calculated from the ion-pair model is obtained if a frequency factor appropriate to the orientation vibrations of the solvent molecules (~10^{11} s^{-1} if frequency dispersion is neglected) is used. The use of a solvent libration frequency rather than kT/h for the preexponential factor appears justified for the ruthenium systems considered here because the inner-sphere barriers are very small, and consequently almost all of the activation energy arises from the solvent reorganization.

Crystal and Molecular Structures of Decamethylmanganocene and Decamethylferrocene. Static Jahn–Teller Distortion in a Metallocene

Derek P. Freyberg, John L. Robbins, Kenneth N. Raymond,* and James C. Smart

Contribution from the Department of Chemistry, University of California, Berkeley, California 94720. *Received June 28, 1978*

Abstract: The crystal and molecular structures of bis(pentamethylcyclopentadienyl)manganese(II) and -iron(II) have been determined by single-crystal X-ray diffraction. The crystal packing of the two compounds is closely related and highly ordered, allowing a detailed comparison of structural parameters. Both metallocenes contain planar, staggered Me_5Cp rings. The ferrocene corresponds to a molecular symmetry of D_{5d} with average Fe–C and C–C distances of 2.050 (2) and 1.419 (2) Å, respectively. The low-spin manganocene has an orbitally degenerate $^2E_{2g}$ ground state in D_{5d} symmetry. This degeneracy is relieved in the solid state by (1) a distortion of the Cp rings in which C–C ring distances range from 1.409 (2) to 1.434 (2) Å and (2) a small slippage of the top and bottom halves of the metallocene "sandwich" to give Mn–C bond lengths which range from 2.105 (2) to 2.118 (2) Å. In both structures the methyl groups bend away from the metal atom 0.06 Å from the Cp rings. Orange crystals of $(C_5(CH_3)_5)_2Mn$ conform to the space group $C2/c$ with a = 15.143 (4) Å, b = 12.248 (3) Å, c = 9.910 (3) Å, and β = 93.56 (3)°. For 2581 independent reflections with $F_o^2 > 3\sigma(F_o^2)$, R = 3.6%, R_w = 5.0%. Orange crystals of $(C_5(CH_3)_5)_2Fe$ conform to the space group $Cmca$ with a = 15.210 (3), b = 11.887 (2), and c = 9.968 (2) Å. For 1217 independent reflections with $F_o^2 > 3\sigma(F_o^2)$, R = 3.9% and R_w = 5.5%. Both structures have four molecules per unit cell with C_i (Mn) and C_{2h} (Fe) crystallographic site symmetry, respectively.

Introduction

Previous structural investigations of metallocenes have demonstrated the dependence of the metal-to-(ring carbon) distance [R(M–C)] on the spin state of the molecule. Manganocene [$(\eta$-$C_5H_5)_2Mn$ or Cp_2Mn] possesses a high-spin $^6A_{1g}$ ($[e_{2g}^2a_{1g}^1e_{1g}^2]$) electronic configuration in benzene solution[1] and in the vapor phase.[2] Bünder and Weiss[3] have determined the structure of solid Cp_2Mn, which is polymeric, while a gas-phase electron diffraction[4] study yielded an R(Mn–C) of 2.383 (3) Å. This is an exceptionally long metal to ring bond when compared to other metallocenes of the first transition series, where R(M–C) ranges from 2.064 (3) Å for Cp_2Fe to 2.280 (5) Å for Cp_2V.[5] Magnetic susceptibility, EPR,[6] and UV photoelectron[2] studies of 1,1′-dimethylmanganocene [$(MeCp)_2Mn$] have demonstrated a thermal equilibrium between high-spin ($^6A_{1g}$) and low-spin ($^2E_{2g}$, $[e_{2g}^3a_{1g}^2]$) electronic configurations, with the high-spin form predominating at elevated temperatures. A gas-phase electron diffraction investigation similarly revealed the presence of two isostructural species in the vapor at 100 °C, with average R(M–C)s of 2.433 (8) and 2.144 (12) Å.[5] Comparison of these bond lengths with the bond length observed in the high-spin Cp_2Mn led to the conclusion that the former distance represents high-spin and the latter low-spin $(MeCp)_2Mn$. An unusually large Mn–C vibrational amplitude (0.160 Å) was noted for low-spin $(MeCp)_2Mn$, and it was concluded that this was a manifestation of a dynamic Jahn–Teller distortion involving ring-tilting modes. The $^2E_{2g}$ configuration is orbitally degenerate; thus in theory the low-spin manganocene is subject to

0002-7863/79/1501-0892$01.00/0

Table I. Summary of Crystal Data for $(Me_5Cp)_2M$, M = Mn, Fe

complex	Mn	Fe
molecular formula	$Mn(C_5(CH_3)_5)_2$	$Fe(C_5(CH_3)_5)_2$
mol wt, g mol^{-1}	325.4	326.3
space group	$C2/c$	$Cmca$
cell constants[a]		
a, Å	15.143 (4)	15.210 (3)
b, Å	12.248 (3)	11.887 (2)
c, Å	9.910 (3)	9.968 (2)
β, deg	93.56 (3)	
cell volume, Å^3	1835 (2)	1802 (1)
formula units/cell, Z	4	4
calcd density, g cm^{-3}	1.18	1.20
absorption coefficient, cm^{-1}	6.8	8.3
color	orange	orange
crystal dimensions	0.3 × 0.4 × 0.7 mm	0.3 × 0.4 × 0.5 mm

[a] Ambient temperature of 23 °C; Mo $K\alpha_1$ radiation, λ = 0.709 30 Å.

Jahn-Teller distortion from pentagonal symmetry. Such a dynamic distortion has been inferred from EPR spectra of low-spin Cp_2Mn and $(MeCp)_2Mn$ in diamagnetic host lattices.[7]

Two of us recently reported the synthesis and magnetic properties of decamethylmanganocene $[(\eta\text{-}C_5(CH_3)_5)_2Mn$ or $(Me_5Cp)_2Mn]$.[8] A temperature-independent magnetic moment of 2.18 ± 0.1 μ_B was found in the range 4.6-313 K, indicating a low-spin ($S = {}^1/_2$) electronic configuration. Subsequent EPR investigations have shown that $(Me_5Cp)_2Mn$, like low-spin $(MeCp)_2Mn$, has a $^2E_{2g}$ ground state.[9] As these molecules are isoelectronic, it might be expected that structural parameters, such as metal to ring distances and distortions from axial symmetry, should also be comparable. To test this hypothesis, the structure of $(Me_5Cp)_2Mn$ was determined by single-crystal X-ray diffraction. The structure of the d^6, closed-shell $(Me_5Cp)_2Fe$ was also determined, to provide a "benchmark" compound. While the latter structural determination was in progress, Struchkov et al.[10] reported the structures of $(Me_4Cp)_2Fe$ and $(Me_5Cp)_2Fe$. Certain features of their solution for $(Me_5Cp)_2Fe$ led us to the conclusion that it was in error, and we report what we believe to be the correct structure.

Experimental Section

$(Me_5Cp)_2Mn$ and $(Me_5Cp)_2Fe$ were prepared by previously described procedures;[8,9,11] slow cooling of hexane solutions afforded single crystals suitable for X-ray crystallography. Since $(Me_5Cp)_2Mn$ is air sensitive, solutions and solids were manipulated using standard Schlenk techniques under an argon atmosphere. Hexane was dried and made oxygen-free by distillation from sodium benzophenone ketyl. Crystals of $(Me_5Cp)_2Mn$ were mounted in quartz capillaries inside an inert-atmosphere glovebox. The capillaries were temporarily sealed with silicone grease inside the box, then torch sealed in the air.

Unit Cell and Diffraction Data. For each crystal, preliminary cell dimensions were obtained by using the program SEARCH[12] to obtain the positions of 25 reflections. Laue symmetry of $2/m$ was observed for $(Me_5Cp)_2Mn$, with hkl $h + k = 2n$, and $h0l$, $l = 2n$. Choice of the centric space group $C2/c$ was confirmed by the structure analysis. For $(Me_5Cp)_2Fe$, Struchkov et al.[10] originally reported the acentric space group $C222_1$, in which the ferrocene has C_2 point symmetry. The structure actually has an additional mirror plane and conforms to the centric space group $Cmca$, in which the ferrocene has C_{2h} crystallographic site symmetry. Crystal data, obtained by a least-squares fit to the setting angles of 22 accurately centered, high-angle reflections, are given in Table I.

Intensity data were collected on an Enraf-Nonius CAD-4 automated diffractometer controlled by a PDP-8/E computer, using monochromatic Mo $K\alpha$ radiation. The intensities of a duplicate set of reflections ($+h$, $\pm k$, $\pm l$ for $(Me_5Cp)_2Mn$; $+h$, $+k$, $\pm l$ for $(Me_5Cp)_2Fe$) with $2° < 2\theta < 70°$ were measured, using the θ-2θ scan technique. The θ scan angle was calculated as $(0.65 + 0.347 \tan \theta)°$ for each crystal, and an aperture with a height of 4 mm and a variable width [width (mm) = 2.5 + 1.0 tan θ for Mn, 2.0 + 1.0 tan θ for Fe] was located 173 mm from the crystal. The scan time was variable, with a maximum of 100 s. The intensities of three standard reflections [(6,0,0), (0,8,0), and (0,0,4) for Mn; (4,0,0), (0,2,0), and (0,0,2) for Fe] were monitored every 7200 s of X-ray exposure, and showed no significant fluctuations. Three orientation standard reflections were monitored every 200 reflections for Mn, every 250 for Fe, and showed no change in setting angles greater than 0.1° in any axis. An attenuator, decreasing the intensity of the diffracted beam by a factor of 18.17, was inserted into the beam when the prescan indicated an intensity too high for accurate counting ($I > 50\,000$ counts/s).

The data (5742 for Mn, 2633 for Fe) were reduced to F^2 and $\sigma(F^2)$ as previously described,[12,13] and then averaged to give 3184 independent reflections for Mn (R factor for averaging 1.6%) and 1558 independent reflections for Fe (R factor for averaging 3.0%). The parameter p, introduced to prevent overweighting of the strong reflections,[14] was set at 0.03 for Mn and 0.04 for Fe. Lorentz and polarization corrections were made, but neither decomposition nor absorption corrections were considered necessary.

Solution and Refinement of the Structures. Manganese. The position of the manganese atom was deduced from the pseudo-face-centering evidenced by the intensities. The positions of several of the ring carbon atoms were assigned from a sharpened Patterson map, and these led to location of all nonhydrogen atoms by standard difference Fourier and least-squares techniques.[15-18] At this point, the methyl hydrogens were clearly visible in a difference Fourier. After anisotropic refinement of the nonhydrogen atoms, the methyl hydrogens were introduced as rigid groups (C-H distance 0.98 Å, bond angle 109.5°) centered on the methyl carbons, with only the rotation angle about the (ring carbon)-(methyl carbon) vector and a group temperature factor being allowed to vary. An extinction coefficient[19] was also refined, as low-angle, high-intensity data had shown systematic lowering of F_o. Full-matrix least-squares refinement with 108 variables, and using the 2581 reflections with $F_o^2 > 3\sigma(F_o^2)$, led to convergence with R = 3.6%, R_w = 5.0%, and the error in an observation of unit weight of 2.08.

No peaks of intensity greater than 0.2 e$^-$ Å^{-3} were seen in a final difference Fourier. Table II gives the positional and anisotropic thermal parameters for the nonhydrogen atoms, while the derived positional and isotropic thermal parameters of the methyl hydrogens are given in Table IX.[29] Root mean square amplitudes of vibration for the nonhydrogen atoms are given in Table VII.[29]

Iron. The position of the iron atom was deduced from the pseudo-face-centering evidenced by the intensities. Initial positions for the carbon atoms were obtained from those of ref 10, by transforming the cell to the standard setting and origin of $Cmca$. Positions of equivalent atoms were then averaged, and the average positions used as starting positions for the refinement. After anisotropic refinement of the nonhydrogen atoms, the methyl hydrogens were introduced as rigid groups and refined in the same way as the Mn complex. An extinction coefficient was also refined. Full-matrix least-squares refinement with 60 variables, and using the 1217 reflections with $F_o^2 > 3\sigma(F_o^2)$, led to convergence with R = 3.9%, R_w = 5.5%, and the error in an observation of unit weight of 1.70.

No peaks of intensity greater than 0.2 e$^-$ Å^{-3} were seen in a final difference Fourier. Table III gives the positional and anisotropic thermal parameters for the nonhydrogen atoms, while the derived positional and isotropic thermal parameters for the methyl hydrogens are given in Table X.[29] Root mean square amplitudes of vibration for the nonhydrogen atoms are given in Table VIII.[29]

Results and Discussion

General Structure. Both $(Me_5Cp)_2Mn$ and $(Me_5Cp)_2Fe$ are planar metallocenes with staggered configurations of the rings. A representative view of the geometry is shown in Figure 1. As shown in Figures 2 and 3, the crystal packing of both compounds is substantially the same and involves rows of metallocene molecules of one orientation alternating along the c direction with rows whose pentagonal axes are nearly perpendicular to the first. Along the b direction, the orientations of the pentagonal axes are constant, but there is alternation

Table II. Positional and Anisotropic Thermal Parameters for the Nongroup Atoms of $(Me_5Cp)_2Mn$

atom	x	y	z	β_{11}[a]	β_{22}	β_{33}	β_{12}	β_{13}	β_{23}
Mn	0.25	0.25	0	37.8 (1)	50.9 (2)	71.5 (3)	3.5 (1)	8.9 (1)	3.1 (2)
C_1	0.1639 (1)	0.3576 (1)	0.0955 (2)	50.4 (7)	73 (1)	103 (1)	17.1 (7)	12.4 (8)	−5 (1)
C_2	0.2048 (1)	0.2855 (2)	0.1918 (1)	54.2 (8)	69.6 (9)	81 (1)	5.2 (8)	17.5 (8)	−2 (1)
C_3	0.2973 (1)	0.3006 (2)	0.1945 (1)	52.4 (8)	78 (1)	87 (1)	5.9 (8)	2.2 (8)	−8 (1)
C_4	0.3140 (1)	0.3840 (1)	0.0979 (2)	56.7 (8)	71 (1)	119 (2)	−9.8 (8)	18 (1)	−18 (1)
C_5	0.2310 (1)	0.4183 (1)	0.0377 (2)	75 (1)	55 (1)	96 (1)	7.1 (8)	18 (1)	−1 (1)
C_6	0.0659 (2)	0.3715 (2)	0.0655 (2)	56 (1)	145 (2)	201 (3)	39 (1)	16 (1)	−2 (2)
C_7	0.1574 (2)	0.2090 (2)	0.2815 (2)	80 (1)	106 (2)	116 (2)	3 (1)	40 (1)	19 (2)
C_8	0.3643 (2)	0.2440 (2)	0.2882 (3)	72 (1)	139 (3)	121 (2)	14 (1)	−24 (1)	−2 (2)
C_9	0.4039 (2)	0.4295 (2)	0.0711 (3)	71 (1)	116 (2)	215 (3)	−34 (1)	29 (2)	−32 (2)
C_{10}	0.2175 (2)	0.5066 (2)	−0.0662 (2)	133 (2)	64 (1)	139 (2)	17 (1)	19 (2)	20 (1)

[a] The anisotropic thermal parameters have been multiplied by 10^4. The form of the anisotropic thermal ellipsoid is $\exp[-(\beta_{11}h^2 + \beta_{22}k^2 + \beta_{33}l^2 + 2\beta_{12}hk + 2\beta_{13}hl + 2\beta_{23}kl)]$.

Table III. Positional and Anisotropic Thermal Parameters for the Nongroup Atoms of $(Me_5Cp)_2Fe$

atom	x	y	z	β_{11}[a]	β_{22}	β_{33}	β_{12}	β_{13}	β_{23}
Fe	0	0	0	33.8 (9)	54.7 (3)	70.2 (5)	0	0	−2.9 (3)
C_1	0	−0.1691 (3)	0.0375 (3)	82 (2)	54 (2)	88 (2)	0	0	3 (2)
C_2	0.0754 (1)	−0.1183 (2)	0.0954 (2)	52.2 (9)	81 (1)	104 (2)	16.8 (9)	5 (1)	12 (2)
C_3	0.0466 (1)	−0.0358 (2)	0.1885 (2)	46.3 (8)	75 (1)	82 (2)	0.0 (9)	−9 (1)	2 (1)
C_4	0	−0.2627 (3)	−0.0628 (4)	156 (4)	65 (2)	110 (4)	0	0	−16 (3)
C_5	0.1695 (2)	−0.1516 (3)	0.0683 (4)	64 (1)	162 (3)	205 (4)	52 (2)	9 (2)	20 (3)
C_6	0.1030 (2)	0.0353 (3)	0.2778 (2)	72 (1)	133 (2)	112 (3)	−14 (2)	−31 (2)	−5 (2)

[a] The anisotropic thermal parameters have been multiplied by 10^4. The form of the anisotropic thermal ellipsoid is $\exp[-(\beta_{11}h^2 + \beta_{22}k^2 + \beta_{33}l^2 + 2\beta_{12}hk + 2\beta_{13}hl + 2\beta_{23}kl)]$.

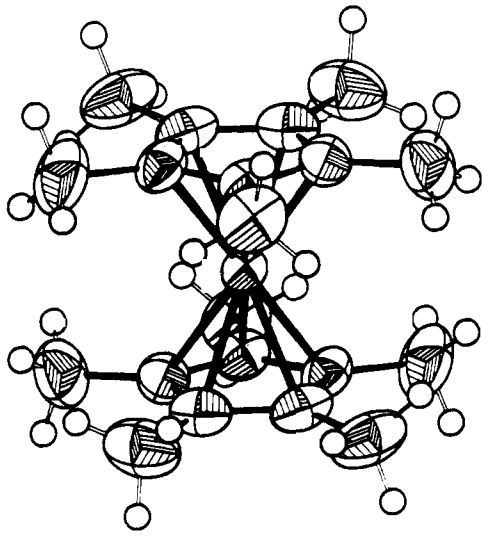

Figure 1. ORTEP drawing of $(Me_5Cp)_2Mn$. The nonhydrogen atoms are drawn at 50% probability contours of the thermal motion. The hydrogen atoms have an arbitrary size.

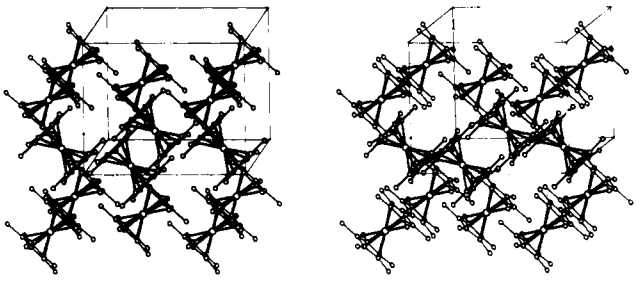

Figure 2. Stereoscopic packing diagram of $(Me_5Cp)_2Mn$, with the unit cell edges shown. b is horizontal, c is vertical, while a is into the paper.

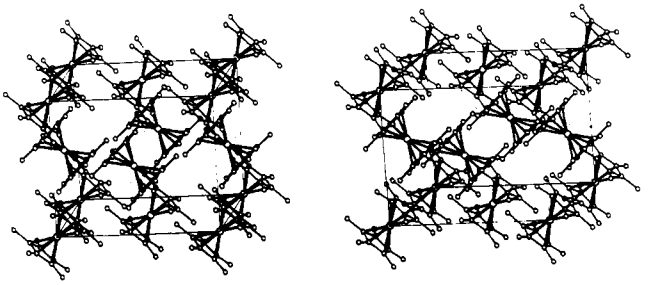

Figure 3. Stereoscopic packing diagram of $(Me_5Cp)_2Fe$, with the unit cell edges shown. The orientation is the same as that of Figure 2.

from x to $x + \frac{1}{2}$ along the rows. For the iron structure there are mirror planes at $x = 0$ which pass through the molecule, whose crystallographic site symmetry is C_{2h}. For the manganese structure, although the packing is nearly the same, there are subtle changes in the methyl orientations that occur in going from the *Cmca* to the $C2/c$ structure.[30] As seen in Table I, the cell constants of the two structures are very similar. *The high crystal quality and close relationship of these structures provide an unusually good opportunity for detailed comparisons of structural parameters.*

Bond distances and angles of both molecules are given in Tables IV and V, respectively, with reference to the atom numbering schemes depicted in Figure 4. The (ring C)–(ring C) distances in $(Me_5Cp)_2Fe$ are all identical within experimental error. The mean value, 1.419 (2) Å, is close to the corresponding distances in Cp_2Fe [1.40 (2) Å][20] and $(Me_4Cp)_2Fe$ [1.428 (4) Å].[9] In addition, the average (ring C)–(methyl C) distance, 1.502 (3) Å, is appropriate for a normal C sp^2–C sp^3 bond, 1.505 (5) Å.[21] The average R(Fe–C) is 2.050 (2) Å, and again this distance is comparable to the

Table IV. Bond Distances in $(Me_5Cp)_2M$, M = Mn, Fe

bond	dist, Å	bond	dist, Å	bond	dist, Å
$Mn-C_1$	2.118 (2)			$Fe-C_1$	2.045 (3)
	[1.216 (3)][a]				[1.199 (4)]
$Mn-C_2$	2.105 (2)	$Mn-C_5$	2.118 (2)	$Fe-C_2$	2.049 (2)
	[1.194 (3)]		[1.217 (3)]		[1.206 (3)]
$Mn-C_3$	2.107 (2)	$Mn-C_4$	2.112 (2)	$Fe-C_3$	2.053 (2)
	[1.197 (3)]		[1.206 (3)]		[1.212 (3)]
	av[b]	2.112 (3)		av	2.050 (2)
		[1.206 (5)]			[1.207 (3)]
C_1-C_2	1.414 (2)	C_1-C_5	1.409 (2)	C_1-C_2	1.419 (3)
C_2-C_3	1.411 (2)	C_4-C_5	1.421 (3)	C_2-C_3	1.419 (3)
C_3-C_4	1.434 (2)			C_3-C_3''	1.418 (4)
	av	1.418 (4)		av	1.419 (2)
C_1-C_6	1.506 (3)			C_1-C_4	1.495 (5)
C_2-C_7	1.504 (3)	C_5-C_{10}	1.498 (3)	C_2-C_5	1.509 (3)
C_3-C_8	1.497 (3)	C_4-C_9	1.508 (3)	C_3-C_6	1.497 (3)
	av	1.504 (2)		av	1.502 (3)

[a] Distances in square brackets represent "in-plane" distances, the distances from the projection of the M atom on the ring plane to the ring carbons. [b] The esd of the mean is the larger of the two given by (1) $\sigma^2(\bar{x}) = \Sigma(x_i - \bar{x})^2/[n(n-1)]$ or (2) $\sigma^2(\bar{x}) = 1/\Sigma(1/\sigma_i^2)$. The mean in each case is the weighted mean.

Table V. Bond Angles in $(Me_5Cp)_2M$, M = Mn, Fe

atoms	angle, deg	atoms	angle, deg	atoms	angle, deg
C_1-Mn-C_2	39.11 (7)	C_1-Mn-C_5	38.86 (7)	C_1-Fe-C_2	40.57 (7)
C_1-Mn-C_3	65.89 (7)	C_1-Mn-C_4	65.70 (7)	C_1-Fe-C_3	68.22 (10)
C_1-Mn-C_2'	140.89 (7)	C_1-Mn-C_5'	141.14 (7)	C_1-Fe-C_2'	139.43 (7)
C_1-Mn-C_3'	114.11 (7)	C_1-Mn-C_4'	114.30 (7)	C_1-Fe-C_3'	111.78 (10)
C_2-Mn-C_3	39.15 (6)	C_4-Mn-C_5	39.25 (7)	C_2-Fe-C_3	40.49 (8)
C_2-Mn-C_4	65.83 (7)	C_3-Mn-C_5	66.07 (7)	C_2-Fe-C_3''	68.06 (8)
C_2-Mn-C_5	65.44 (7)			C_2-Fe-C_2''	68.09 (11)
C_2-Mn-C_3'	140.85 (6)	C_4-Mn-C_5'	140.75 (7)	C_2-Fe-C_3'	139.51 (8)
C_2-Mn-C_4'	114.17 (7)	C_3-Mn-C_5'	113.93 (7)	C_2-Fe-C_3'''	111.94 (8)
C_2-Mn-C_5'	114.56 (7)			C_2-Fe-C_2'''	111.91 (11)
C_3-Mn-C_4	39.74 (7)			C_3-Fe-C_3''	40.43 (10)
C_3-Mn-C_4'	140.26 (7)			C_3-Fe-C_3'''	139.57 (10)
$Mn-C_1-C_2$	69.95 (9)	$Mn-C_1-C_5$	70.58 (9)	$Fe-C_1-C_2$	69.86 (13)
$Mn-C_1-C_6$	127.5 (1)			$Fe-C_1-C_4$	127.5 (2)
$Mn-C_2-C_1$	70.93 (8)	$Mn-C_5-C_1$	70.55 (9)	$Fe-C_2-C_1$	69.6 (1)
$Mn-C_2-C_3$	70.50 (9)	$Mn-C_5-C_4$	70.13 (9)	$Fe-C_2-C_3$	69.9 (1)
$Mn-C_2-C_7$	126.8 (1)	$Mn-C_5-C_{10}$	126.5 (1)	$Fe-C_2-C_5$	128.9 (2)
$Mn-C_3-C_2$	70.35 (9)	$Mn-C_4-C_5$	70.62 (9)	$Fe-C_3-C_2$	69.6 (1)
$Mn-C_3-C_4$	70.31 (9)	$Mn-C_4-C_3$	69.95 (9)	$Fe-C_3-C_3''$	69.79 (5)
$Mn-C_3-C_8$	127.4 (1)	$Mn-C_4-C_9$	126.8 (1)	$Fe-C_3-C_6$	128.7 (2)
$C_2-C_1-C_5$	107.9 (1)			$C_2-C_1-C_2''$	107.9 (2)
$C_2-C_1-C_6$	126.0 (2)	$C_5-C_1-C_6$	125.9 (2)	$C_2-C_1-C_4$	126.1 (1)
$C_1-C_2-C_3$	108.8 (2)	$C_1-C_5-C_4$	108.3 (1)	$C_1-C_2-C_3$	108.1 (1)
$C_1-C_2-C_7$	125.7 (2)	$C_1-C_5-C_{10}$	126.1 (2)	$C_1-C_2-C_5$	125.6 (2)
$C_3-C_2-C_7$	125.4 (2)	$C_4-C_5-C_{10}$	126.1 (2)	$C_3-C_2-C_5$	126.2 (2)
$C_2-C_3-C_4$	107.3 (1)	$C_3-C_4-C_5$	107.6 (1)	$C_2-C_3-C_3''$	108.0 (1)
$C_2-C_3-C_8$	125.6 (2)	$C_5-C_4-C_9$	126.9 (2)	$C_2-C_3-C_6$	127.0 (2)
$C_4-C_3-C_8$	127.0 (2)	$C_3-C_4-C_9$	125.4 (2)	$C_3''-C_3-C_6$	125.0 (1)

distances found in Cp_2Fe [2.04 (2) Å][20,22] and $(Me_4Cp)_2Fe$ [2.054 (3) Å].[10]

The average R(Mn-C) in $(Me_5Cp)_2Mn$ is 2.114 (2) Å, about 0.3 Å shorter than the corresponding distance in high-spin $(MeCp)_2Mn$ [2.433 (8) Å][5] and Cp_2Mn [2.383 (3) Å].[4] The value is, however, very close to that determined for low-spin $(MeCp)_2Mn$, 2.144 (12) Å.[5] The contraction of the metal-ring distance in low-spin manganocenes can be rationalized on the basis of the molecular orbital diagram for high- and low-spin metallocene d^5 systems. In the $^6A_{1g}$ configuration, three electrons occupy the bonding e_{2g} and nonbonding a_{1g} levels and two electrons occupy the antibonding e_{1g} level. The electronic configuration of the low-spin manganocenes, $^2E_{2g}$, has been established by EPR spectroscopy.[6,9] In this configuration, all five 3d electrons reside in the e_{2g} and a_{1g} levels, leaving the antibonding e_{1g} level vacant [see Figure 5 for the electronic configurations of $(Me_5Cp)_2Mn$ and $(Me_5Cp)_2Fe$]. A net increase in the formal metal-ring bond order is expected, and the foreshortening of the bond is not surprising. Haaland[5] has advanced similar arguments to explain the relative metal to ring distances observed in neutral metallocenes of the first transition series. Assuming that the e_{2g} and a_{1g} levels are bonding between metal atom and rings while the e_{1g} level is antibonding, Haaland defines the "metallocene electron imbalance", n, as the sum of the number of electrons in the e_{1g} level plus the number of vacancies in the e_{2g} and a_{1g} levels. Thus $n = 0$ for Cp_2Fe, $n = 1$ for Cp_2Co and low-spin manganocenes, $n = 2$ for Cp_2Cr and Cp_2Ni, $n = 3$ for

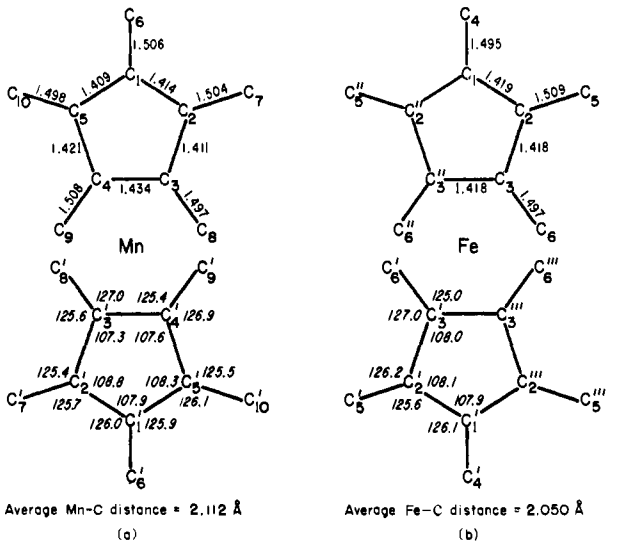

Figure 4. Labeling diagram for $(Me_5Cp)_2Mn$ (a) and $(Me_5Cp)_2Fe$ (b), showing some bond distances and angles. The unprimed atoms are those refined (coordinates x, y, z); the singly primed are those related by an inversion center $(-x, -y, -z)$ in both the Mn and Fe complexes; the doubly primed are those related by the mirror plane $(-x, y, z)$; and the triply primed are those related by the twofold axis $(x, -y, -z)$.

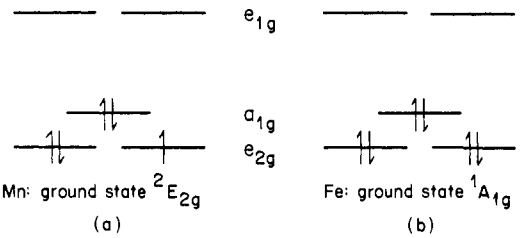

Figure 5. Energy level diagram for $(Me_5Cp)_2Mn$ (a) and $(Me_5Cp)_2Fe$ (b).

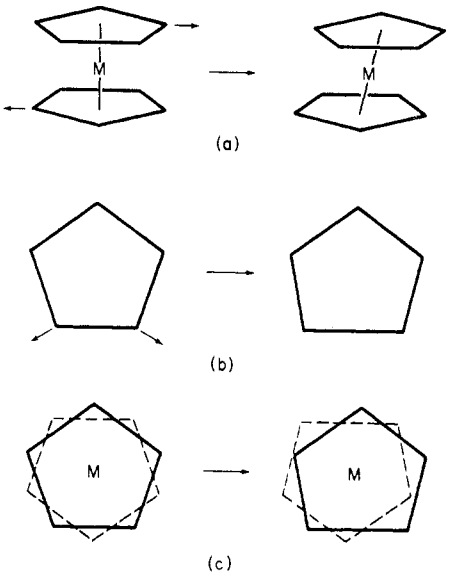

Figure 6. The principal modes of Jahn–Teller distortion in $(Me_5Cp)_2Mn$: (a) ring slippage (concerted rotation); (b) intra-ring distortion; and (c) the resulting distortion observed in $(Me_5Cp)_2Mn$ in the solid state.

Table VI. Least-Squares Planes for $(Me_5Cp)_2M$, M = Mn, Fe

complex		Mn		Fe
atoms in plane		C_1, C_2, C_3, C_4, C_5		$C_1, C_2, C_3, C_3'', C_2''$
coefficients of plane[a]	A	1.6092		0
	B	−8.5314		−8.1746
	C	−7.0839		7.2369
	D	−3.4643		1.6568
distances from plane, Å	C_1	0.0003	C_1	0.0026
	C_2	−0.0004	C_2	−0.0009
	C_3	0.0003	C_3	0.0003
	C_4	−0.0001	C_3''	0.0003
	C_5	−0.0002	C_2''	−0.0009
	Mn	1.7338	Fe	1.6568
	C_6	−0.0624	C_4	−0.0360
	C_7	−0.0593	C_5	−0.0765
	C_8	−0.0725	C_6	−0.0650
	C_9	−0.0538	C_6''	−0.0650
	C_{10}	−0.0389	C_5''	−0.0765
av deviation from plane, Å		0.0003		0.0010
av deviation of methyl carbons, Å		−0.057 (12)		−0.064 (17)

[a] The planes are expressed in the form $Ax + By + Cz = D$, in which x, y, and z are fractional coordinates and D is the distance from the plane to the origin in Å.

Cp_2V, and $n = 5$ for high-spin Cp_2Mn. The R(M–C)s of these complexes, as determined by X-ray crystallography and electron diffraction, are found to increase monotonically with n. By this formalism, the R(M–C) of $(Me_5Cp)_2Mn$ is expected to be somewhat greater than that of $(Me_5Cp)_2Fe$, as here. Haaland's model also predicts that the R(M–C)s of Cp_2Co and the low-spin manganocenes should be comparable. The R(M–C) of Cp_2Co as determined by X-ray crystallography, 2.096 (8) Å,[3] and electron diffraction, 2.119 (3) Å,[23] is indeed similar to our value for $(Me_5Cp)_2Mn$.

The position and orientation of the methyl groups in these decamethylmetallocenes merit comment. As was found in $(Me_4Cp)_2Fe$,[10] the alkyl groups are about 0.06 Å above the plane (directed away from the metal) defined by the C_5 rings (see Table VI). This is in contrast to the situation in unsubstituted metallocenes where the C–H bonds are directed below the ring plane (toward the metal atom).[24] As can be seen in Figure 1, the methyl groups in $(Me_5Cp)_2Mn$ are each oriented in a fashion which directs two hydrogens below the plane of the ring and one above, approximately perpendicular to the ring plane. The situation in $(Me_5Cp)_2Fe$ is similar, except that the C_6 methyl groups are rotated to bring one C–H bond approximately into planarity with the ring.

For a single Me_5Cp^- ring, an expected methyl orientation might be a "gear mesh" configuration in which one H of each methyl group is coplanar with the ring and equidistant from two of the hydrogens on an adjacent group. Examination of space-filling models of the $(Me_5Cp)_2M$ molecule reveals a variety of potential alkyl group orientations which minimize inter-ring or intra-ring methyl interactions while allowing free rotation of methyl groups and Me_5Cp rings. The configuration we observe seems to be the one which maximizes H–H distances between rings.

The closest H–H distances (adjacent methyl groups) within one ring in $(Me_5Cp)_2Fe$ range from 2.15 to 2.66 Å (average = 2.4 Å). Between rings, the closest H–H distances range from 2.49 to 3.41 Å (average = 2.6 Å). In $(Me_5Cp)_2Mn$, intra-ring H–H distances range from 2.16 to 2.54 Å (average = 2.3 Å), while inter-ring distances range from 2.56 to 2.97 Å (average = 2.7 Å).

Thus hydrogens on adjacent methyl groups of the same ring are 0.2–0.4 Å closer than hydrogens on nearest-neighbor methyl groups on opposing rings. If the deviation of the alkyl groups from the ring plane is a result of steric effects, it is probably due to steric interactions of methyl groups within

each ring, since in a molecule with only one Me_5Cp ring, $(Me_5Cp)Fe(CO)_2SO_2CHCH_2C_6H_5$,[25] the methyl carbons were also found to lie 0.025–0.191 Å above the ring plane.

Static Jahn–Teller Distortion. As described in the Introduction, a metallocene such as $(Me_5Cp)_2Mn$ in the $^2E_{2g}$ state possesses an orbitally degenerate electronic configuration subject to Jahn–Teller distortion. Deviations from pure axial (D_{5d}) symmetry by either a static or dynamic mechanism would serve to lift the degeneracy of the $^2E_{2g}$ ground state. While evidence for a dynamic distortion in low-spin $(MeCp)_2Mn$ and Cp_2Mn has been presented,[5,7] we find in the structure of $(Me_5Cp)_2Mn$ indications of a static distortion which involves primarily distortion of the Cp ring through changes in the C–C bond lengths.

Examination of the bond lengths in Table IV reveals two discrepancies between the structures of $(Me_5Cp)_2Mn$ and $(Me_5Cp)_2Fe$. First, the metal–(ring C) distances in $(Me_5Cp)_2Mn$ vary from 2.105 to 2.118 Å, reflecting a difference of 0.013 Å (6σ) from closest to most distant ring carbon. By comparison, in $(Me_5Cp)_2Fe$, the prototype metallocene not subject to Jahn–Teller distortion, these distances vary by only 0.008 Å ($<4\sigma$). This type of distortion, marginal in the manganese complex, is illustrated in Figure 6a. The distortion may be envisioned as a ring slippage with C_4 and C_5 (and C_4', C_5') moving away from the metal while C_2 and C_3 move toward the metal. Alternatively, this may be viewed as a symmetric ring tilt, a recognized vibrational mode (E_{1g}) for metallocenes.[26] While the metal–C distances vary significantly in $(Me_5Cp)_2Mn$, the rings themselves remain essentially planar.

The second, and major, distortion of the manganocene structure occurs in the Cp ring itself. In the $(Me_5Cp)_2Fe$ structure, the (ring C)–(ring C) distances do not deviate significantly from the mean of 1.419 Å. However, as seen in Table IV, these distances range from 1.409 (2) to 1.434 (2) Å in $(Me_5Cp)_2Mn$. This distortion is exaggerated in Figure 6b. The C_3–C_4 bond expands while the C_2–C_3 and C_1–C_5 bonds contract relative to the idealized bond distance of 1.419 Å. The net result of these two distortions is depicted in Figure 6c, in a projection view.

EPR studies on orbitally degenerate d^5 and d^7 metallocenes have shown that the unpaired electron in these systems is substantially delocalized over the ring π orbitals.[7,27] Since the Cp rings share part of the radical character of these molecules, the variation of ring carbon distances may in part reflect a Jahn–Teller distortion of the Me_5C_5 ring. Recent calculations by Bischof[28] indicate that Jahn–Teller distortions in the C_5H_5 radical would result in a variation of (ring carbon)–(ring carbon) bond lengths yielding a C_5 ring of local C_{2v} symmetry.

Unusually large metal–C vibrational amplitudes in the gas-phase structures of Cp_2Co[23] and low-spin $(MeCp)_2Mn$[5] were interpreted as structural evidence for a dynamic Jahn–Teller distortion in these molecules. In this study, root mean square amplitudes of vibration for the atoms of $(Me_5Cp)_2Mn$ and $(Me_5Cp)_2Fe$ were found to be comparable (Tables VII, VIII). This evidence discounts the importance of dynamic distortions in solid $(Me_5Cp)_2Mn$.

Summary

In conclusion, the close structural relationship of $(Me_5Cp)_2Mn$ and $(Me_5Cp)_2Fe$ allows detailed comparison of their structural parameters. The ferrocene has a regular D_{5d} molecular symmetry in which the Me_5Cp rings are staggered. The low-spin manganocene exists in an orbitally degenerate ground state, $^2E_{2g}$, in D_{5d} symmetry. In the solid what appears to be a static Jahn–Teller distortion to lower symmetry is observed, which relieves the degeneracy. This involves primarily changes in ring C–C bond lengths—which range from 1.409 (2) to 1.434 (2) Å. Accompanying this is a smaller distortion which involves the parallel movement of the top and bottom halves of the "sandwich" in opposite directions. To our knowledge, this is the first observation of such a Jahn–Teller distortion in an organometallic compound.

Acknowledgment. This research was supported by the National Science Foundation. We thank Dr. Edgar C. Baker for his assistance in the preliminary diffraction studies.

Supplementary Material Available: Tables VII–XII, comprising root mean square amplitudes of vibration, derived positional and isotropic thermal parameters for the methyl hydrogen atoms, and observed and calculated structure factors for $(Me_5Cp)_2Mn$ and $(Me_5Cp)_2Fe$ (30 pages). Ordering information is given on any current masthead page.

References and Notes

(1) Wilkinson, G.; Cotton, F. A.; Birmingham, J. M. *J. Inorg. Nucl. Chem.* **1956**, *2*, 95–113.
(2) Evans, S.; Green, M. L. H.; Jewitt, B.; King, G. H.; Orchard, A. F. *J. Chem. Soc., Faraday Trans. 2* **1974**, 356–376. Evans, S.; Green, M. L. H.; Jewitt, B.; Orchard, A. F.; Pygall, C. F. *ibid.* **1972**, 1847–1865.
(3) Bünder, W. Dissertation, Universität Hamburg, 1974. Cited, with figure, in ref 7, p 308.
(4) Almenningen, A.; Haaland, A.; Motzfeldt, T. "Selected Topics in Structure Chemistry", Universitetsforlaget: Oslo, 1967; p 105.
(5) Almenningen, A.; Haaland, A.; Samdal, S. *J. Organomet. Chem.* **1978**, *149*, 219–229.
(6) Switzer, M. E.; Wang, R.; Rettig, M. F.; Maki, A. H. *J. Am. Chem. Soc.* **1974**, *96*, 7669–7674. Ammeter, J. H.; Bucher, R.; Oswald, N. *Ibid.* **1974**, *96*, 7833–7835.
(7) Ammeter, J. H. *J. Magn. Reson.* **1978**, *30*, 299–325.
(8) Smart, J. C.; Robbins, J. L. *J. Am. Chem. Soc.* **1978**, *100*, 3936.
(9) Robbins, J. L.; Smart, J. C.; Edelstein, N. Manuscript in preparation.
(10) Struchkov, Yu. T.; Andrianov, V. G.; Sal'nikova, T. N.; Lyatifov, I. R.; Materikova, R. B. *J. Organomet. Chem.* **1978**, *145*, 213–223.
(11) King, R. B.; Bisnette, M. B. *J. Organomet. Chem.* **1967**, *8*, 287–297.
(12) The Enraf–Nonius FORTRAN IV system operates the CAD-4 diffractometer. In addition to locally written programs for the CDC 7600, the following programs or modifications were used: Zalkin's FORDAP Fourier program; Ibers' NUCLS, a group least-squares version of the Busing–Levy ORFLS program; ORFFE, a function and error program by Busing and Levy; ORTEP 2, by Johnson; and RBANG, a program to handle rigid groups.
(13) Duesler, E. N.; Raymond, K. N. *Inorg. Chem.* **1971**, *10*, 1486–1492.
(14) Baker, E. C.; Brown, L. D.; Raymond, K. N. *Inorg. Chem.* **1975**, *14*, 1376–1379.
(15) Definitions of the indicators are $R = \Sigma|F_o - F_c|/\Sigma|F_o|$ and $R_w = [\Sigma w(F_o - F_o)^2/\Sigma w|F_o|^2]^{1/2}$; the error in an observation of unit weight is $[\Sigma w(F_o - F_c)^2/(N_o - N_v)]^{1/2}$, where N_o is the number of observations and N_v the number of variables.
(16) Cromer, D. T.; Mann, B. *Acta Crystallogr., Sect. A* **1968**, *24*, 321–325.
(17) Stewart, R. F.; Davidson, E. T.; Simpson, W. T. *J. Chem. Phys.* **1965**, *42*, 3175–3187.
(18) Cromer, D. T. *Acta Crystallogr.* **1963**, *18*, 17–23.
(19) Zachariasen, W. H. *Acta Crystallogr.* **1963**, *16*, 1139–1144
(20) Dunitz, J. D.; Orgel, L. E.; Rich, A. *Acta Crystallogr.* **1956**, *9*, 373–375.
(21) Sutton, L. E., Ed. "Tables of Interatomic Distances and Configuration in Molecules and Ions." Supplement 1956–1959, Chemical Society: London, 1965; p S15*s*.
(22) A gas-phase electron diffraction study yielded a more precise value, 2.064 (3) Å. See ref 4.
(23) Almenningen, A.; Gard, E.; Haaland, A.; Brunvoll, J. *J. Organomet. Chem.* **1976**, *107*, 273–279.
(24) Haaland, A. *Top. Curr. Chem.* **1975**, *53*, 1–23.
(25) Churchill, M. R.; Wormald, J. *Inorg. Chem.* **1971**, *10*, 572–578.
(26) Nakamoto, K. "Infrared Spectra of Inorganic and Coordination Compounds", Wiley-Interscience: New York, N.Y., 1970; p 271.
(27) Ammeter, J. H.; Swalen, J. *J. Chem. Phys.* **1972**, *57*, 678–701.
(28) Bischof, P. *J. Am. Chem. Soc.* **1977**, *99*, 8145–8149.
(29) Tables VII–X will appear in the microfilm edition. See paragraph at end of paper for ordering supplementary material.
(30) NOTE ADDED IN PROOF. The low-temperature structure of $(Me_5Cp)_2Mn$ is also *Cmca* with a somewhat altered distortion that is yet similar to that observed here.